WORLD JOURNAL OF PHARMACEUTICAL AND MEDICAL RESEARCH
www.wjpmr.com

SIGNIFICANT METABOLOMIC DIFFERENCES BETWEEN THE TUMOR AND NON-TUMOR ADJACENT MUCOSA IN COLORECTAL CANCER - A TARGETED MASS-SPECTROMETRY-BASED STUDY TO IDENTIFY POTENTIAL BIOMARKERS

Marcos Vinicius ARAUJO Denadai*[1, 2], Carlos Augusto Rodrigues Veo[1, 2], Sandra Morini Silva[2],M. Gordian Adam[3], Udo Muller[3], Simon Schafferer[3], Ismael D C G Da Silva,[4] Isabella Alves Brunetti[5] and Delcio Matos[1,6]

[1]Health Evidence-Based Postgraduate Program– Escola Paulista de Medicina, Sao Paulo Federal University, São Paulo, Brazil.
[2]Barretos Cancer Hospital, Fundação Pio XII, Barretos, SP, Brazil.
[3]Biocrates Life Sciences AG, Innsbruck, Austria.
[4]Department of Gynecology and Obstetrics– Escola Paulista de Medicina, Sao Paulo Federal University, São Paulo, Brazil.
[5]LEEA- Laboratory of Ecotoxicology and Pesticide Efficacy.
[6]UNIMES - Santos Metropolitan University, Santos, SP, Brazil.

*Corresponding Author: Marcos Vinicius ARAUJO Denadai
Health Evidence-Based Postgraduate Program– Escola Paulista de Medicina, Sao Paulo Federal University, São Paulo, Brazil.
DOI: 10.20959/wjpmr20207-3693

ABSTRACT

Metabolomics is an emerging analytical tool that has allowed cancer research to elucidate specific biomarkers and helped improve clinical outcomes. The aim of the project was to identify metabolic conditions in patients with colorectal cancer. A targeted metabolomic approach with the Biocrates Absolute *IDQ*® p180 Kit was used to quantify metabolites of various biochemical classes. The samples comprised 85 human cancer tissue and 85 cancer-surrounding tissue samples from the same patients. Classes of amino acids, biogenic amines, acylcarnitines, glycerophospholipids, sphingolipids and monosaccharides were analyzed. The statistical analysis included data normalization and quality control, Principal Component Analysis (PCA), Hierarchical Cluster Analysis (HCA), univariate statistics with significance testing, and analysis of fold changes. The main biochemical pathways affected were also analyzed. Univariate statistical analysis by comparing tumor and tumor-surrounding tissue found a total of 118 significantly altered metabolites. Tumor tissue samples displayed severely altered metabolomic features, which affected different pathophysiological pathways ranging from energy to lipid metabolism. Metabolomic reprogramming, glutaminolysis, prominent Warburg Effect, and increased IDO activity, which all have been described for cancer cells, could be conclusively observed in this analysis. The importance of lipid alterations occurring in tumor cells were also confirmed with this study. In colorectal cancer, the tumor and tumor-surrounding tissue present distinct metabolomic states and dramatic metabolomic reprogramming. Especially the role of sphingomyelins and lysophosphatidylcholines (lysoPCs) as potential tissue biomarkers for colorectal cancer needs further investigation.

KEYWORDS: Colorectal cancer; biomarkers; spectrometry-based.

INTRODUCTION

Colorectal cancer is the third leading cause of cancer related death in the USA. To improve clinical outcomes and facilitate personalized therapies, sensitive molecular tools are needed to help identify novel biomarkers for metabolic pathway aberrations. Metabolomics is an emerging analytical tool that can be described as the systematic study of the entire profile of small molecules in a clinical sample that are detected using mass spectrometry. Analysis of metabolites from a multitude of matrices, such as tumor tissue and adjacent mucosa, may represent the downstream functional products of gene expression and protein synthesis, all of which influence colorectal cancer carcinogenesis.[1]

The diagnostic power for metabolomic tests for colorectal neoplasia can be improved using a multimodal approach and combining metabolites from diverse chemical classes. In addition, quantification of metabolites enhances separation of disease-specific metabolomic profiles. Future efforts must be focused on developing quantitative assays for the metabolites comprising the optimal diagnostic biomarker.[2]

Da Silva et al., in 2018, identified consistent metabolic changes with inborn-like errors and defined a continuum from normal controls of elevated risk for invasive breast cancer and other adenocarcinomas. The findings describe a new early detection method and the assessment of

prognosis platform for glandular cancer as well as support a role for pre-existingin born-like errors of metabolism in the process of adenocarcinoma carcinogenesis. A novel concept of glandular carcinogenesiswas defined, particularly in breast cancer, that characterizes malignant transformation as the manifestation of underlying metabolic insufficiencies.[3]

To investigate colorectal cancer metabolism, an electronic literature search was performed by Fan Z et al., from 1998 to January 2016, for studies that evaluate the metabolomic profile of patients with colorectal cancer regarding diagnosis, recurrence and prognosis. Altered metabolites and pathways were related to prognosis, survival, and recurrence. This review could represent the most comprehensive information and summary about metabolism to date. It certificates that metabolomics have enormous potential for both discovering clinical biomarkers and elucidating previously unknown mechanisms of colorectal cancer pathogenesis.[4]

The aim of our project was to identify metabolomics changes mass-spectrometry-based in tumor tissue and tumor-adjacent mucosa in patients with colorectal adenocarcinoma.

MATERIAL AND METHODS

Study samples
The samples included 85 human cancer tissue and 85 cancer-surrounding tissue samples from the same patients. Patients with a scheduled colorectal resection after a CRC diagnosis were recruited for this study. All patients provided informed written consent and a research plan was approved by the Barretos Cancer Hospital – FPio XII Ethics Committee. The patients undergoing chemo and/or radiotherapy prior to surgery were excluded from the study. Sample collection: within 30 min of surgery, a 5-mm section of CRC and adjacent mucosal tissue samples that were >10 cm proximal to the CRC were collected from resected colons in the Pathology Lab. Clinicopathological data was collected including information on the patient (age, gender, relapse, survival), as well as tumor sample characteristics (tumor site, differentiation grade, venous invasion, lymph node invasion, perineural invasion, peritumoral infiltration, TNM stage, AJCC staging), see Table 1. Human tissue samples were stored immediately at -80 °C following collection until processed for metabolomics. Collection was verified by the study technician who was present in the pathology lab and pre-op room for each resection. Patient-matched CRC and adjacent mucosa were collected for all individuals. All samples were shipped to Biocrates Life Sciences AG, Innsbruck, Austria for metabolomics and statistical data analyses.

Metabolite profiling
To extract metabolites from tissue and tumour tissue, samples were homogenized using Precellys® with ethanol phosphate buffer. For metabolite measurements, samples were centrifuged and the supernatant was used for analysis. A Biocrates Absolute *IDQ*® p180 Kit was used to quantify metabolites of various biochemical classes including amino acids, biogenic amines, acylcarnitines, glycerophospholipids, sphingolipids, and monosaccharides. The p180 kit is a widely used targeted metabolomics platform that yields highly reproducible results.[5] The fully automated assay was based on PITC (phenylisothiocyanate) derivatization in the presence of internal standards followed by FIA-MS/MS (Flow injection analysis tandem mass spectrometry) to detect acylcarnitines, (lyso-) phosphatidylcholines, sphingomyelins, and hexoses, and LC-MS/MS (liquid chromatography tandem mass spectrometry) to detect amino acids and biogenic amines, using a SCIEX 4000 QTRAP® (SCIEX, Darmstadt, Germany) or a Waters XEVO™ TQMS (Waters, Vienna, Austria) instrument with electrospray ionization (ESI). The experimental metabolomics measurement technique is described in detail by patent US 2007/0004044.[6] For the quantification of the LC−MS/MS part, the metabolite concentrations were calculated by stable isotope dilution and seven-point calibration curves. For the FIA-MS/MS part, metabolites were quantified using a one-point internal standard calibration; they were isotope-corrected as well. The amount of tissue used for the analysis was included in the concentration calculations to yield absolute concentration values in pmol/mg tissue.

Statistical Analysis

Different statistical methods were applied with the aim of identifying differences in metabolite levels between cancer tissue and cancer surrounding tissues. The analysis included data normalization and quality control, Principal Component Analysis, Hierarchical Cluster Analysis, univariate statistics with significance testing, and analysis of fold changes. In addition, the main biochemical pathways affected were analyzed. The workflow of the analysis is summarized in Figure 1. The results of the second part of this study, involving plasma samples of colorectal cancer patients, will be published separately.

Data cleaning, imputation, and transformation

To exclude analytes in which concentration values are missing or are below the limit of detection (LOD), a general cleaning of the data set was performed. The cleaned data set was then further used for scaling, transformation, and the statistical analysis.[7] The concentration values for the whole dataset were cleaned focusing on the tissue type as group variable, applying an 80% rule. For statistical analysis at least 80% valid values above LOD needed to be available per analyte in the samples for each tissue type. If at least one group - be it the cancer tissue or the non-cancerous adjacent mucosa - fulfilled this criterion the analyte was included for further statistical analysis. Therefore, if an analyte had 20% or more values below LOD in both groups, it was excluded.

Missing value imputation is commonly used to logically replace missing values with a non-zero value while maintaining the overall data structure. Remaining values below LOD in the data set were, therefore, imputed applying a log-spline imputation method, which was developed for data being right censored, left censored, or interval censored.[8]

The study data was further processed by a log2 transformation. This transformation is commonly applied to meet assumptions of statistical tests (e.g. symmetric distribution of data, correction for heteroskedasticity, and skewness of the data) and to improve the interpretability and visualization.

Data processing, statistical analysis, and data visualization were performed using R (Version 3.2.3).

Univariate Statistics
General measures of central tendency and dispersion were calculated for the cleaned and imputed data set to provide a quantitative description for the different groups. A paired t-test was performed on the log transformed concentration values to detect significantly altered analytes between cancer tissue and cancer surrounding tissue from the same patients. Finally, fold changes of the analyte changes were calculated.

A significance level of $\alpha = 0.05$ was determined, and p-values were calculated. To control the False-Discovery-Rate (FDR) during multiple comparisons, an adjusted p-value (Benjamini-Hochberg correction) was calculated.[9] All analytes with significantly altered concentrations ($p < 0.05$) and fold changes are listed in Table 2.

Multivariate Statistics
Multivariate statistical methods were applied to not only detect changes of single metabolites between different groups, but also to show the dependency structures between individual analytes. In this case, Principal Component Analysis (PCA), Partial Least Squares Discrimination Analysis (PLS-DA), and Hierarchical Cluster Analysis (HCA) were used as multivariate approaches. The multivariate analysis was performed on the cleaned, imputed, and log-transformed data.

The hypothesis-free PCA was based on an unsupervised linear mixture model to highlight the variance within the dataset while reducing the dimensionality, generating a smaller number of mutually decorrelated principal components (PCs). As a supervised linear mixture model, the PLS regression was employedto separate the predefined groups, the tumor tissue and the non-tumor tissue, as much as possible based on the metabolite concentrations.

An HCA was performed to visualize samples according to intrinsic similarities in their measurements, irrespective of specific sample groupings. Here, the complete-linkage method was applied, which defines the cluster distance between two clusters to be the maximum distance between their individual components.

RESULTS

Metabolite Profiling
All the 170 samples were randomized and measured on three different kit-plates. The results were later normalized based on the quality control level QC2. Accuracy of the measurements was determined assessing the accuracy of the calibrators, which was in the normal range of the method for all analytes. Quality control samples were within the pre-defined tolerances of the method. To test for a potential bias from measuring the samples on different plates, all samples from the three plates were subjected to a PCA (suppl. Figure 1 A, B). The sample distribution was quite homogeneous for the three plates measured, with very few outliers and the Hotelling's T^2 95% confidence ellipses being almost superimposable (suppl. Figure 1A). The corresponding PCA loadings plot (suppl. Figure 1B) shows the analyte distribution, again without outliers or abnormalities. Therefore, no obvious plate effects occurred during the measurement allowing robust statistical analysis of the metabolites.

From the 188 metabolites measured by the kit, 51 were removed during the cleaning process, leaving 137 metabolites for statistical analysis.

Multivariate Statistics: Tumor vs. tumor-surrounding tissue
In an unsupervised multivariate PCA, the samples were clearly separated based on the two individual tissue types with almost no overlap (Figure 2A). This is quite striking, because it indicates that the differences between tumor- and tumor-surrounding tissue were stronger than the inter-individual differences, even thoughthe cohort was very heterogeneous regarding age, gender, BMI, medication, comorbidities, and general lifestyle.

As expected, the separation was even more pronounced in the supervised PLS-DA, with no overlap between the 95% confidence ellipses and only very few outliers (Figure 2B). Together these analyses show that the tumor and tumor-surrounding tissue have distinct metabolomic states due to a dramatic reprogramming of the colon cancer cell metabolism compared to the normal cells.

In line, also the HCA (Figure 3) revealed distinct clustering according to the type of tissue. Furthermore, it is noteworthy that the analytes clustered together according to their ontology class. This indicates that the observed changes between tumor and tumor-surrounding tissue were not random but related metabolites were affected in a similar way. Therefore, we analyzed the metabolites with significantly changed concentrations between cancer and non-cancer tissues focusing on pathways and ontology classes.

Univariate statistics
Comparison of tumor and tumor surrounding tissue from the same patients showed 118 significantly altered metabolites. The significant analytes, together with the p-values and fold changes are listed in supplemental Table 1.

Hexoses and amino acids connected to glycolysis
The three amino acidsalanine, serine, and glycinecan be generated from glycolysis intermediates. Alanine can be generated from pyruvate, serine from 3-phosphoglycerate and glycine from serine. The concentrations of all three glycolysis-related amino acids (as well as their sum) were significantly higher in tumor tissue samples than in the normal adjacent samples (Figure 4). In contrast, average hexose levels, which mainly represent glucose, were significantly lower in tumor tissue. Together, these results point to an overall increased glycolysis rate in the tumor tissue.

Amino acids connected to the tricarboxylic acid (TCA) cycle
The amino acid aspartate can be converted into the TCA metabolite oxaloacetate (and vice versa) and thus is a link between the urea cycle and the TCA cycle, and it acts as a source for asparagine synthesis. The amino acid glutamate can be converted to the TCA metabolite α-ketoglutarate (and vice versa) and acts as a source metabolite for the synthesis of glutamine and proline, which in turn can be hydroxylated to form hydroxyproline. In this study, average concentrations of proline, its hydroxylated form t4-OH-proline, asparagine, and aspartate were significantly higher in cancer tissue (Figure 5). This indicates the increased utilization of amino acids for biosynthesis during tumor growth. Glutamine levels were reduced in the tumor tissue, consistently the ratio for glutaminolysis ((Ala + Asp + Glu) / Gln) was significantly increased.

Amino acids connected to the urea cycle and polyamines
The TCA cycle is connected to the urea cycle via arginine. Both arginine as well as the posttranslationally modified asymmetrically dimethylatedargininine (ADMA) are increased in the tumor tissue. Citrulline, Arginine, and Ornithine are important intermediates of the urea cycle (Figure 6). In this study, the concentrations of all these metabolites were significantly elevated in tumor tissue samples.

Ornithine also acts as a source for Putrescine, which in turn is the source metabolite for spermidine and subsequently spermine synthesis. Both putrescine and spermidine were significantly increased in tumor tissue, while spermine was slightly but significantly reduced (Figure 6C).

Aromatic amino acids
Phenylalanine, tryptophan, and tyrosine form the aromatic amino acids (AAAs). The concentrations of tyrosine, tryptophan, and the sum of the AAAs were augmented in the cancer tissue (Figure 7). Tryptophan acts as a source of serotonin and kynurenine, which were also significantly altered in the cancer tissue.While serotonin was significantly reduced in tumor tissue, kynurenine was increased, indicating that these two pathways downstream of tryptophan were regulated quite differently in the tumor. Consistent with the altered kynurenine and tryptophan levels, the metabolism indicator for indoleamine 2,3-dioxygenase (IDO) activity (ratio of kynurenine / tryptophan) was significantly increased in the samples from colorectal cancer patients.

Essential amino acids
All analyzed essential amino acids, including threonine, lysine, histidine, and methionine, as well as metabolites thereof, such as alpha AAA or taurine, were higher in tumor tissue samples (Figure 9). Again, this indicates the high amount of amino acids present in tumor cells needed for protein biosynthesis and rapid proliferation. In contrast, histamine was decreased in tumor tissue. Histamine is derived from the decarboxylation of histidine.

Branched chain amino acids (BCAAs), which comprise leucine, isoleucine, and valine, are the most abundant essential amino acids. In this study, all single BCAAs analytes as well as their sum were significantly higher in the tumor tissue samples (Figure 8), a common observation previously reported in various cancer tissues.

Acylcarnitines
Acylcarnitines represent the carrier form of activated fatty acids and acetate for the transport across the inner mitochondrial membrane (10). In this study, all acylcarnitineswith significant concentration changes displayed higher levels in tumor tissue (Figure 9). The elevated average levels of carnitine in tumor tissue correlated with the observed increased levels ofthe amino acids it is synthetized from, methionine and lysine.

Phospholipids
We observed a shift in the metabolite levels of different subclasses within the phospholipids. Almost all phosphatidylcholines (except PC aa C36:3, PC aa C36:4, PC ae C34:3, and PC ae C36:5) showed increased concentrations in tumor tissue samples (Figure 10). Oppositely, the levels of the related lysophosphatidylcholines (lysoPCs) (Figure 11) and all sphingomyelins (except SM C16:1) (Figure 12) were significantly decreased in the tissue samples from colorectal cancer patients. These results point to a marked difference in membrane lipid composition between the two groups.

DISCUSSION
In this study, metabolomic differences in tumor tissue and tumor surrounding tissue from patients with colorectal cancer were investigated. Therefore, a targeted metabolomic approach using Biocrates® p180 Kit was

conducted analyzing 170 tissue samples. The overall excellent analyte coverage was the basis for investigating a variety of key biochemical pathways.

We observed statistically significant differences in metabolite concentrations of several different pathways. The glycolysis pathway was one of the pathways in which significant changes were most expected. Most cancer cells rely less on oxidative phosphorylation for energy generation, but instead display increased glycolysis rates, a feature also known as 'Warburg effect'. Warburg observed an elevated glucose uptake in cancer cells, which was considered as the basis of cancer cell metabolism and was subsequently the most used metabolomic feature to distinguish tumor cells from normal cells.[11] Directly connected to this are the increased levels of most amino acids. High amounts of amino acids derived from glycolysis (glycine, serine, and alanine) in the tumor tissue can be used for increased protein biosynthesis during cancer growth and proliferation. In addition, glycine can serve as a precursor for DNA-nucleotide synthesis and is therefore essential for efficient tumor proliferation. The concentrations of amino acids related to the TCA cycle were increased in the colorectal cancer patient tissues as well, as their utilization is augmented to support tumor growth.The TCA cycle comprises a series of consecutive reactions that form the key part of aerobic respiration in cells and is used to produce energy through the oxidation of Acetyl-CoA, which is derived from the breakdown of carbohydrates, fatty acids, and proteins. In addition, the TCA cycle provides direct precursors for the biosynthesis of certain amino acids.

Glutamine was the only amino acid with significantly reduced concentrations in the tumor tissue. Increased glutaminolysis, which describes the conversion of glutamine to glutamate in tumor tissue, was highly prominent in this study. Apart from glucose, the other main substrate that contributes to energy production in cells is glutamine. Glutaminolysis is upregulated in many types of cancer and glutamine provides the crucial source of nitrogen to rapidly proliferating cells for amino acid synthesis via glutamate production and transamination. In addition, instead of oxidizing glutamine completely to generate ATP, the mitochondria in cancer cells shunt glutamine into citrate for rapid lipid synthesis and NADPH production. As a result of this switch to increased glutamine dependence by the mitochondria, the decreased contribution of glucose to the TCA cycle can be compensated for by contributions from glutamine. This observed mitochondrial reprogramming has been described as resulting from increased expression of the oncogenic Myc transcription factor, which enhances the expression of the Glutaminase enzyme and specific glutamine transporters to support increased glutaminolysis. Chen, J-Q et al., Jin L et al., and Kim MH et al. have written detailed reviews on metabolic reprogramming and glutaminolysis.[12,17]

Table 1: Metabolites with significantly different concentrations comparing tumor tissue and tumor-surrounding normal tissue.Red: concentration reduced in the tumor tissue, Blue: concentration increased in the tumor tissue.

Rank	Metabolite	p-value	p-value (BH adj.)	Mean Fold change		Rank	Metabolite	p-value	p-value (BH adj.)	Mean Fold change
1	H1	4.05E-41	5.54E-39	9.6		60	SM.C16.1	3.31E-11	7.57E-11	-1.3
2	SM.C18.0	7.12E-38	4.88E-36	3.4		61	PC.ae.C38.0	3.52E-11	7.90E-11	-1.2
3	Serotonin	8.93E-37	4.08E-35	14.8		62	PC.ae.C42.2	7.25E-11	1.60E-10	-1.4
4	Pro	7.98E-36	2.73E-34	-3.4		63	Ser	9.11E-11	1.98E-10	-1.5
5	Ile	1.48E-32	4.05E-31	-2.3		64	SM..OH..C22.2	1.51E-10	3.24E-10	1.4
6	Tyr	1.36E-30	3.11E-29	-2.3		65	PC.ae.C32.2	2.14E-10	4.51E-10	-1.7
7	PC.aa.C32.1	1.62E-30	3.17E-29	-2.9		66	PC.aa.C40.5	2.52E-10	5.22E-10	-1.3
8	Thr	2.64E-30	4.52E-29	-2.1		67	PC.ae.C40.1	3.09E-10	6.32E-10	-1.3
9	Leu	2.96E-29	4.50E-28	-2.3		68	PC.ae.C40.3	3.31E-10	6.68E-10	-1.4
10	Phe	6.76E-29	9.26E-28	-2.2		69	Cit	3.90E-10	7.75E-10	-1.7
11	Trp	3.11E-28	3.87E-27	-2.2		70	PC.aa.C40.3	5.31E-10	1.04E-09	-1.4
12	Val	2.36E-27	2.69E-26	-2.0		71	PC.ae.C38.1	6.29E-10	1.21E-09	-1.5
13	PC.aa.C32.2	9.22E-27	9.71E-26	-2.9		72	PC.ae.C36.0	5.05E-09	9.53E-09	-1.3
14	t4.OH.Pro	3.23E-24	3.16E-23	-2.3		73	lysoPC.a.C16.0	5.08E-09	9.53E-09	1.4
15	Kynurenine	1.30E-23	1.19E-22	-3.0		74	PC.ae.C44.6	6.61E-09	1.22E-08	-1.5
16	SM..OH..C22.1	1.84E-23	1.57E-22	1.9		75	PC.ae.C42.1	1.14E-08	2.07E-08	-1.2
17	SM..OH..C16.1	3.99E-23	3.21E-22	1.6		76	SM.C26.1	2.31E-08	4.17E-08	1.4
18	Met	1.25E-21	9.54E-21	-1.9		77	PC.ae.C34.1	4.13E-08	7.34E-08	-1.3
19	lysoPC.a.C16.1	1.41E-21	1.02E-20	-2.3		78	PC.ae.C38.3	4.20E-08	7.38E-08	-1.3
20	His	3.69E-21	2.53E-20	-1.7		79	SM..OH..C24.1	4.43E-08	7.69E-08	1.3
21	Asn	8.67E-21	5.66E-20	-2.1		80	PC.aa.C32.3	8.16E-08	1.40E-07	-1.4
22	SM.C18.1	1.54E-20	9.62E-20	1.6		81	lysoPC.a.C24.0	1.27E-07	2.14E-07	-1.4

|									
23	PC.ae.C44.3	1.02E-19	6.09E-19	-1.7		82	SM..OH..C14.1	1.54E-07	2.57E-07	1.2
24	C0	1.87E-19	1.07E-18	-2.0		83	lysoPC.a.C20.4	2.06E-07	3.40E-07	-1.3
25	Met.SO	2.27E-19	1.25E-18	-3.0		84	PC.ae.C38.2	5.30E-07	8.64E-07	-1.3
26	PC.aa.C42.4	2.65E-18	1.40E-17	-1.6		85	C2	5.50E-07	8.87E-07	-1.5
27	PC.ae.C30.0	4.98E-18	2.53E-17	-2.1		86	lysoPC.a.C26.1	6.94E-07	1.11E-06	-1.2
28	ADMA	1.20E-17	5.86E-17	-2.3		87	lysoPC.a.C17.0	7.83E-07	1.23E-06	1.3
29	C18	1.38E-17	6.51E-17	-2.4		88	lysoPC.a.C18.1	1.16E-06	1.81E-06	-1.4
30	Lys	1.70E-17	7.76E-17	-1.5		89	PC.aa.C30.2	1.66E-06	2.56E-06	-2.0
31	lysoPC.a.C20.3	2.65E-17	1.17E-16	-1.8		90	PC.aa.C28.1	1.72E-06	2.61E-06	-1.2
32	PC.aa.C34.4	2.77E-17	1.18E-16	-1.6		91	PC.aa.C34.2	1.03E-05	1.55E-05	1.1
33	Arg	9.06E-17	3.76E-16	-1.6		92	PC.ae.C38.5	1.19E-05	1.77E-05	1.2
34	PC.aa.C30.0	1.01E-16	4.08E-16	-1.7		93	PC.aa.C34.3	2.98E-05	4.40E-05	-1.2
35	PC.ae.C44.5	1.38E-16	5.39E-16	-1.8		94	PC.ae.C36.5	4.98E-05	7.25E-05	1.2
36	C16	2.20E-16	8.38E-16	-2.3		95	PC.aa.C36.1	1.05E-04	1.51E-04	-1.2
37	Glu	2.66E-16	9.85E-16	-1.7		96	PC.ae.C40.4	1.40E-04	2.00E-04	-1.2
38	C18.2	5.37E-16	1.94E-15	-1.9		97	lysoPC.a.C18.0	2.23E-04	3.16E-04	1.2
39	Ala	1.69E-15	5.93E-15	-1.6		98	Spermidine	2.99E-04	4.14E-04	-1.5
40	SM.C24.1	1.75E-15	5.99E-15	1.6		99	SM.C16.0	2.99E-04	4.14E-04	1.1
41	C18.1	2.29E-15	7.66E-15	-2.1		100	PC.aa.C38.3	3.86E-04	5.29E-04	-1.2
42	PC.ae.C30.1	2.73E-15	8.91E-15	-2.5		101	PC.ae.C34.0	4.41E-04	5.98E-04	-1.2
43	Gly	2.90E-15	9.23E-15	-1.6		102	PC.aa.C38.0	6.07E-04	8.15E-04	-1.1
44	PC.aa.C42.2	4.42E-15	1.38E-14	-1.6		103	Spermine	9.60E-04	1.28E-03	1.1
45	Taurine	5.69E-15	1.73E-14	-1.4		104	Gln	1.35E-03	1.78E-03	1.1
46	PC.aa.C42.1	5.31E-14	1.58E-13	-1.5		105	PC.aa.C38.6	1.42E-03	1.85E-03	-1.1
47	PC.aa.C40.2	5.60E-14	1.63E-13	-1.6		106	Putrescine	1.87E-03	2.42E-03	-1.5
48	PC.ae.C32.1	5.77E-14	1.65E-13	-1.7		107	PC.ae.C40.2	2.03E-03	2.60E-03	-1.2
49	PC.aa.C36.3	5.91E-14	1.65E-13	1.3		108	PC.ae.C34.3	2.71E-03	3.44E-03	1.2
50	Asp	1.75E-13	4.80E-13	-2.0		109	SM.C26.0	4.48E-03	5.63E-03	1.2
51	PC.aa.C36.6	3.77E-13	1.01E-12	-1.4		110	lysoPC.a.C28.0	4.75E-03	5.91E-03	-1.2
52	PC.aa.C42.5	1.02E-12	2.68E-12	-1.4		111	PC.aa.C32.0	7.75E-03	9.57E-03	-1.1
53	C14	1.10E-12	2.84E-12	-2.3		112	PC.ae.C40.5	8.12E-03	9.93E-03	-1.1
54	PC.aa.C36.4	1.69E-12	4.30E-12	1.3		113	alpha.AAA	9.53E-03	1.16E-02	-1.3
55	SM.C20.2	3.19E-12	7.94E-12	2.6		114	PC.ae.C40.6	1.97E-02	2.36E-02	-1.1
56	PC.aa.C40.6	1.03E-11	2.52E-11	-1.3		115	PC.ae.C36.4	2.10E-02	2.48E-02	-1.1
57	PC.aa.C40.4	1.25E-11	3.00E-11	-1.5		116	PC.aa.C36.0	2.10E-02	2.48E-02	-1.1
58	PC.ae.C42.3	1.75E-11	4.13E-11	-1.5		117	lysoPC.a.C28.1	3.32E-02	3.89E-02	-1.1
59	Orn	2.50E-11	5.80E-11	-1.6		118	Histamine	3.40E-02	3.95E-02	1.5
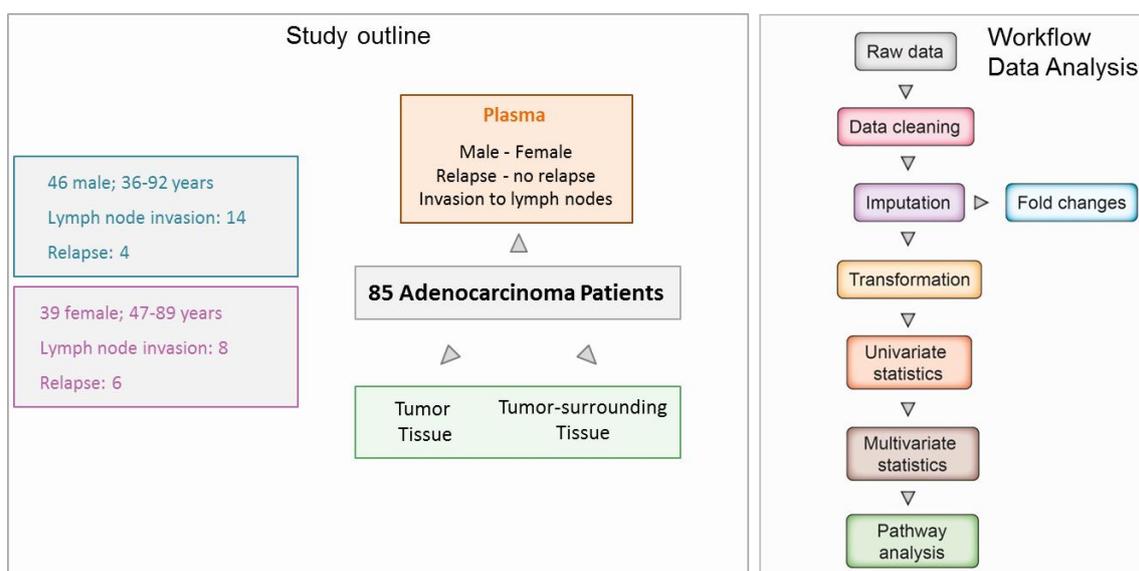
Figure 1: Schematic depiction of the study outline and data analysis workflow
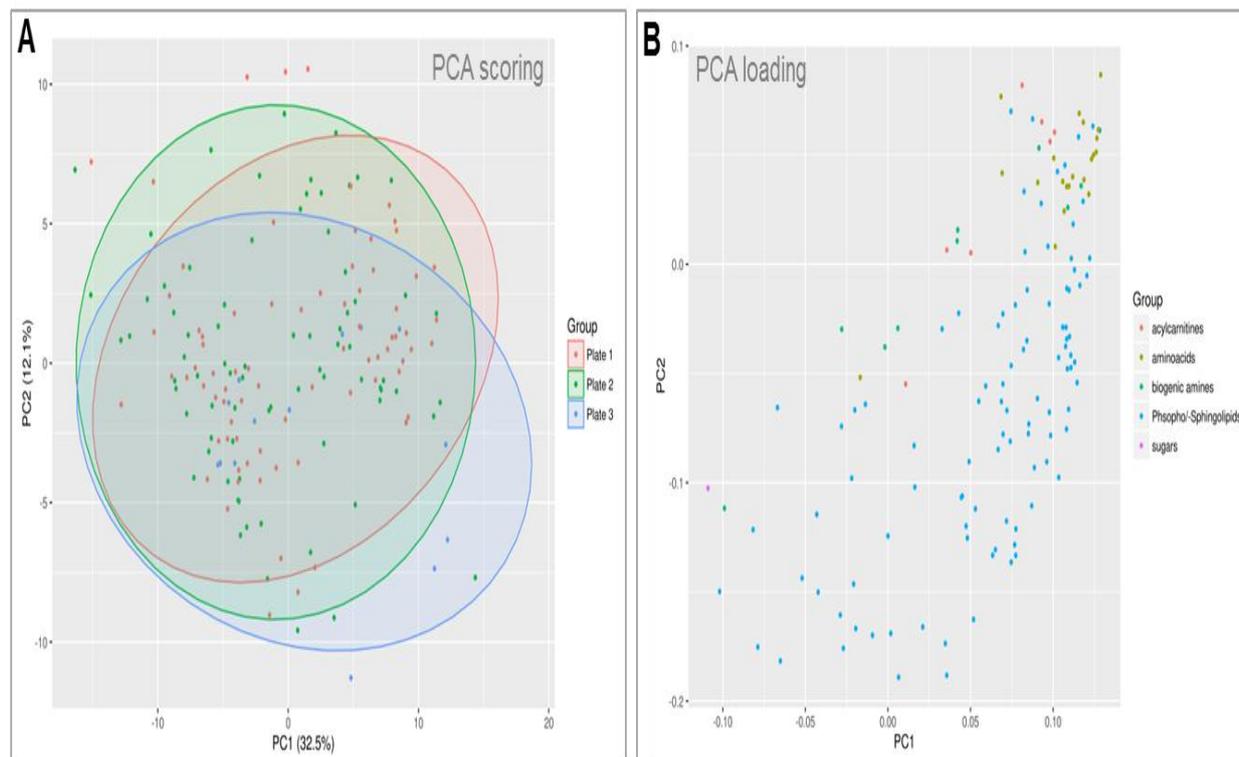
Suppl. Figure 1: Multivariate statistical analysis of plate effects for the tissue samples
PCA scoring (A) and loading (B) were applied on the cleaned, imputed, and log2 transformed data set for the tissue samples over the three measured plates. The 95% confidence interval ellipses are illustrated for the two different groups.
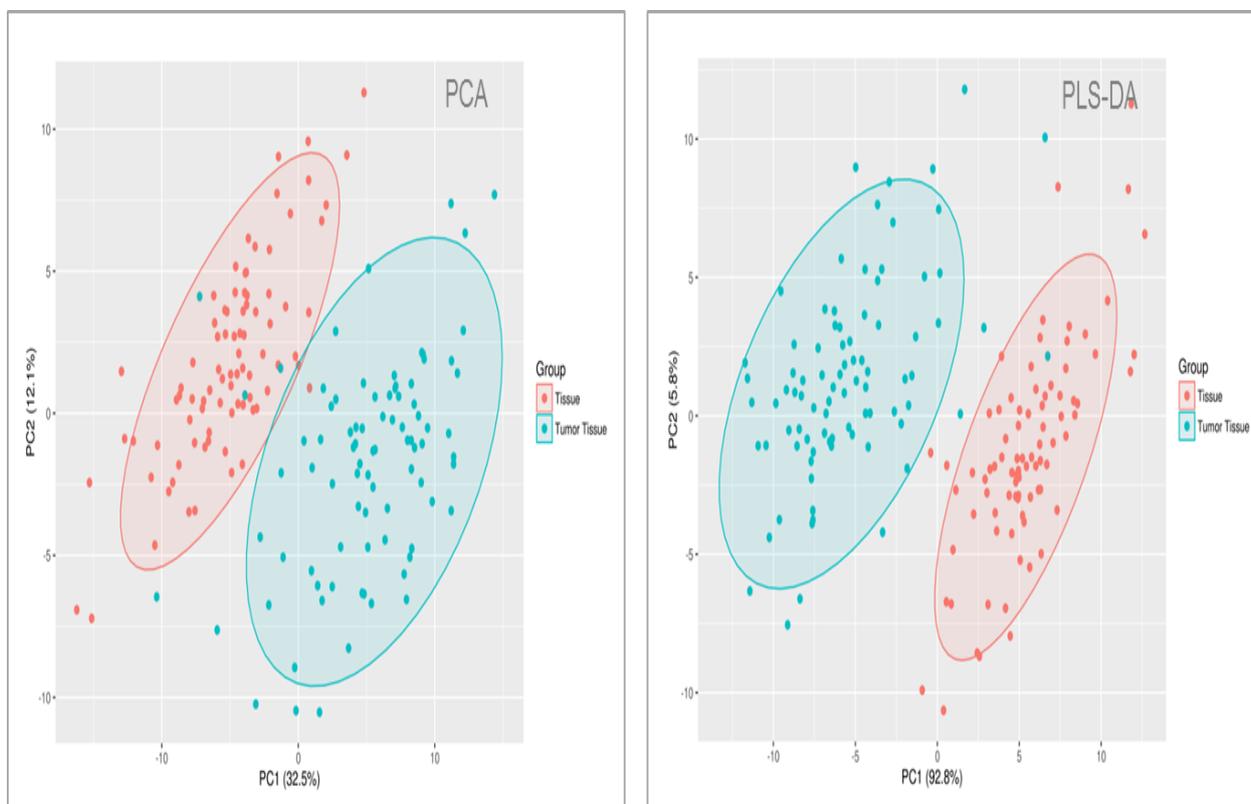

Figure 2: Multivariate statistical analysis for significant analytes between the tumor and tumor-surrounding tissue.
PCA (A), PLS-DA (B) were applied on the cleaned, imputed and log2 transformed data set. The 95% confidence interval ellipses are illustrated for the two different groups.
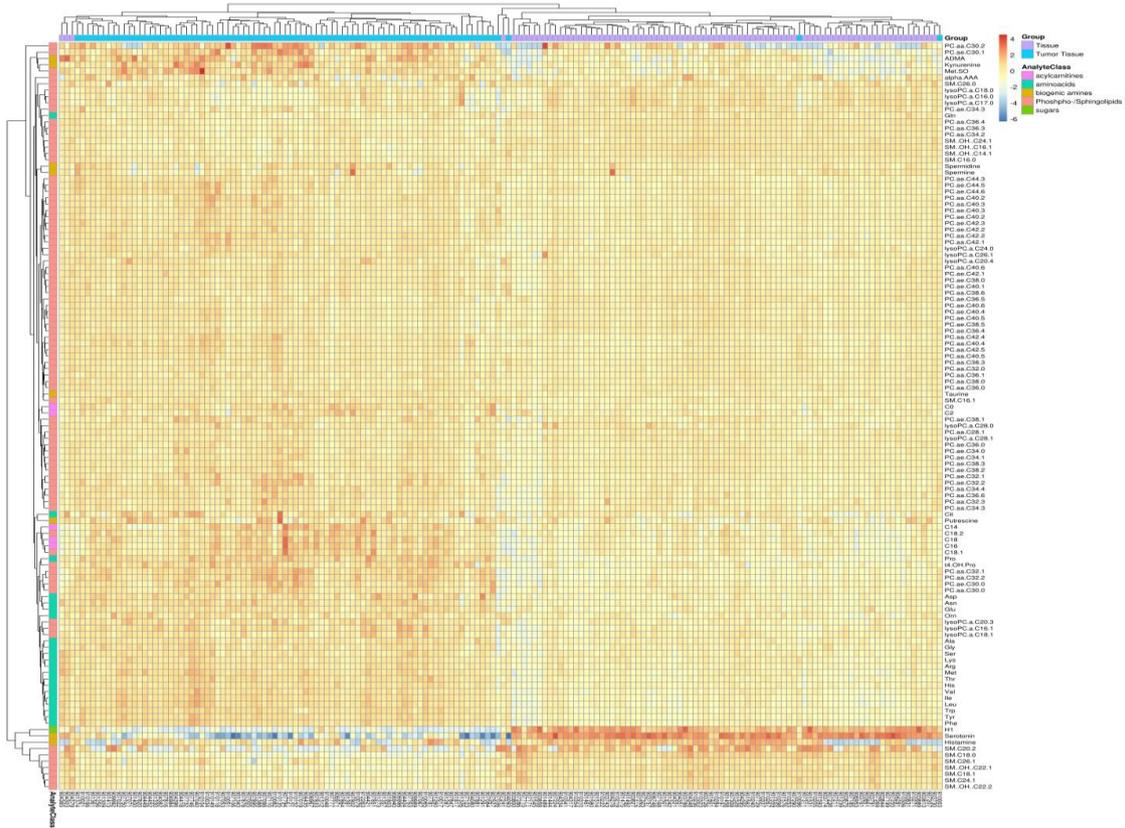
Figure 3: HCA for significant analytes between the tumor and tumor-surrounding tissue
HCA was applied on the cleaned, imputed, and log2 transformed data set. Samples are indicated in the individual columns and significantly altered analytes in the individual rows.
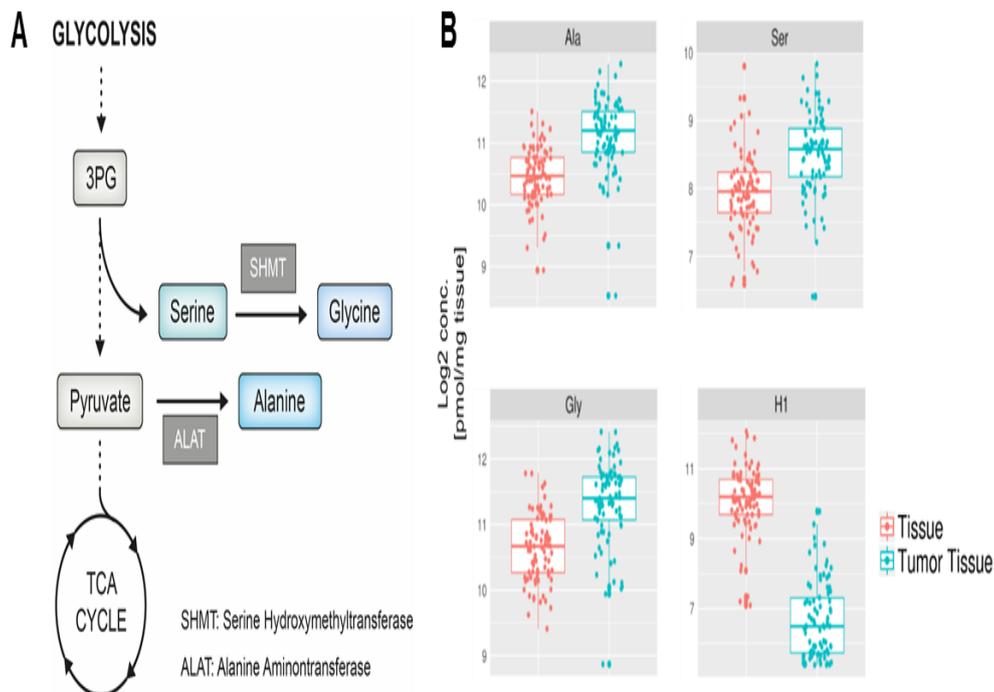
Figure 4: Significantly changed metabolites connected to glycolysis
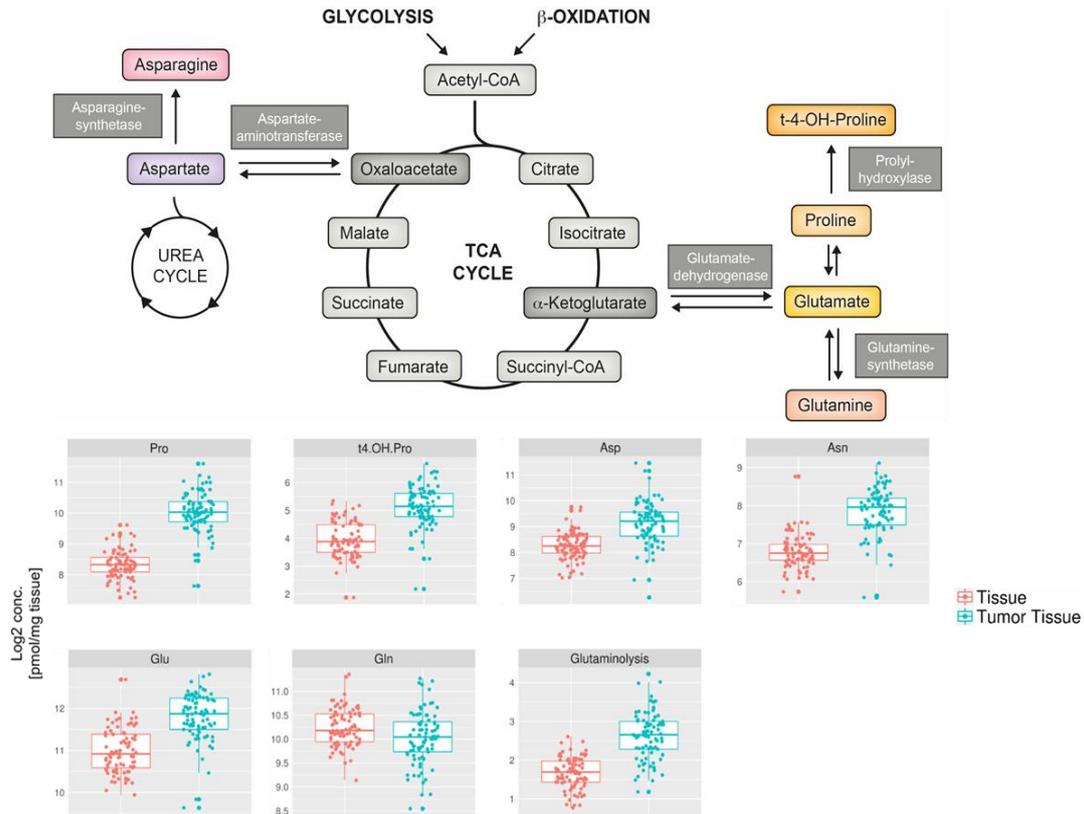**A) Schematic depiction of the origin of glycolysis-derived amino acids. B) Significantly changed analytes between tumor and tumor-surrounding tissue**

Figure 5: Significantly changed metabolites connected to the TCA cycle
A) Schematic depiction of the TCA cycle and associated amino acids. B) Analytes with significantly changed concentrationscomparing tumor and tumor-surroundingtissue, including the ratio for glutaminolysis.
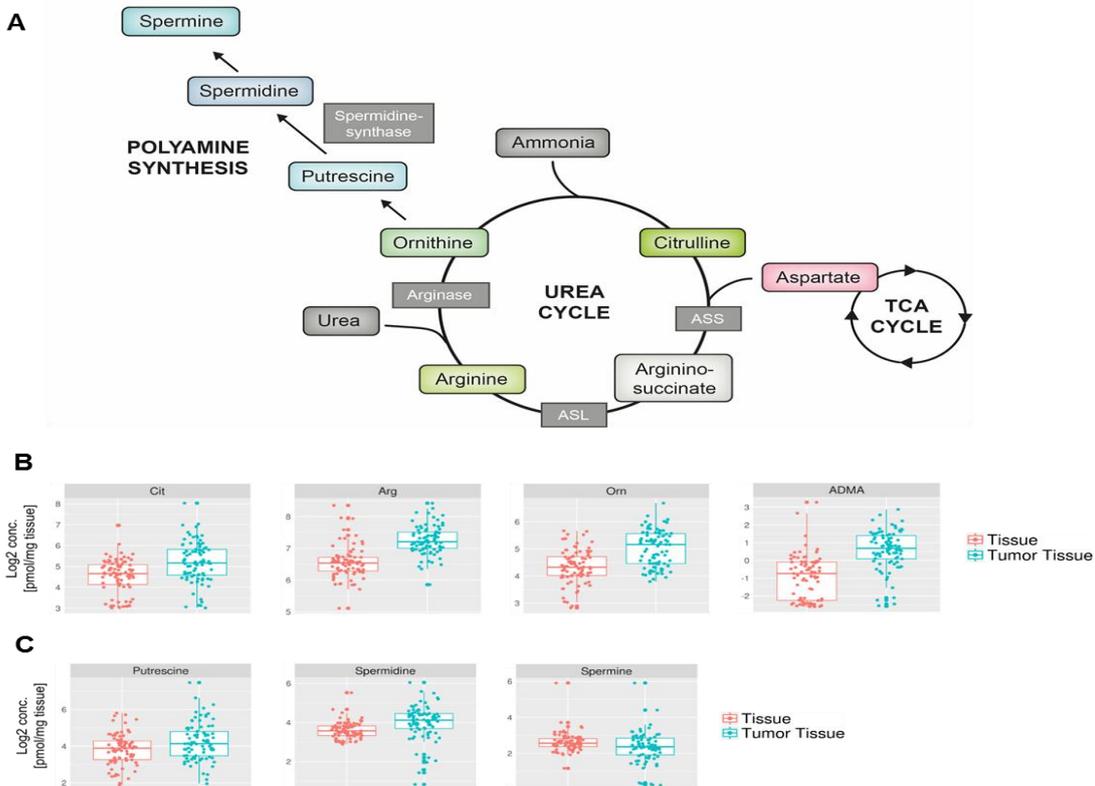
Figure 6: Significantly changed amino acids connected to the urea cycle and polyamines
A) Schematic depiction of the urea cycle and polyamine synthesis. B) Amino acids with significantly changed concentrations between tumor and tumor-surrounding tissue. C) Polyamines with significantly changed concentrations between tumor and tumor-surrounding tissue.
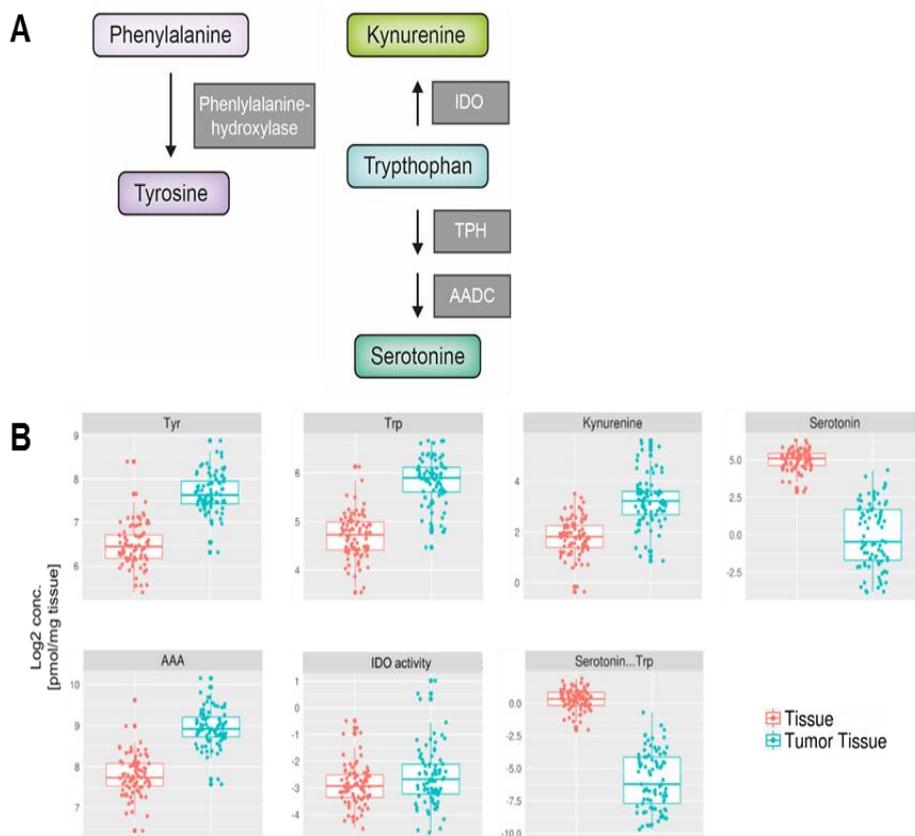
Figure 7: Significantly changed metabolites and ratios connected to aromatic amino acids
A) Schematic depiction of the aromatic amino acids and connected metabolites. B) Analytes with significantly changed concentrations between tumor and tumor-surroundingtissue, including the ratios for kynurenine synthesis (IDO activity) and serotonin synthesis (Serotonin…Trp) from tryptophan.
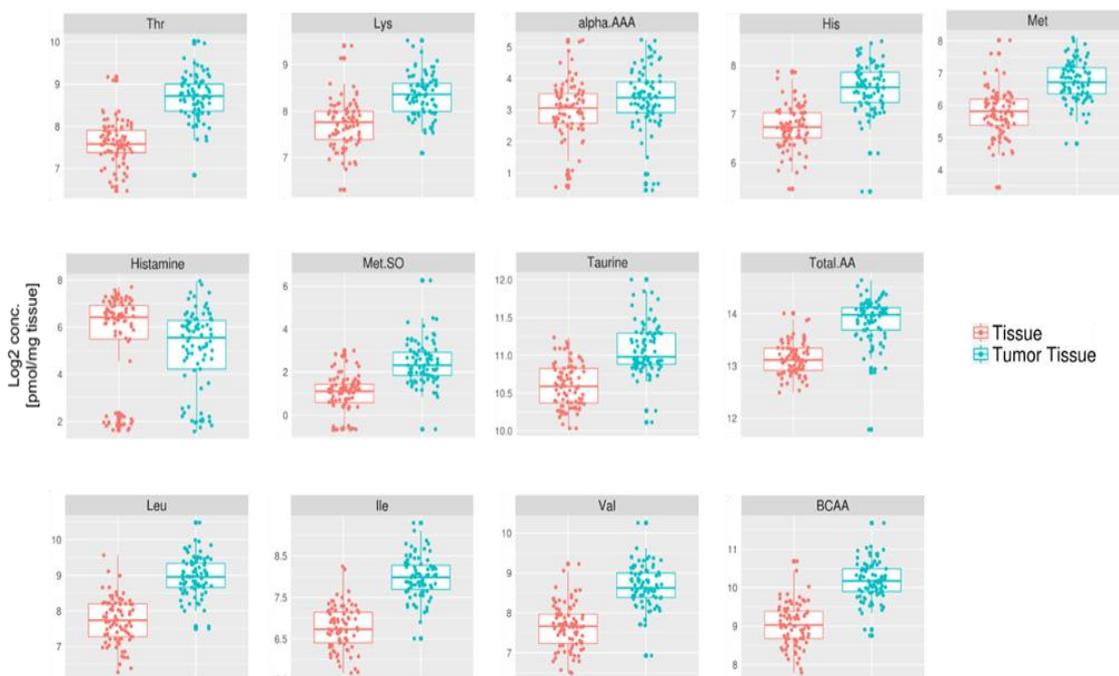

Figure 8: Significantly changed essential amino acids and related metabolites
Analytes with significantly changed concentrations between tumor and tumor-surroundingtissue, including the sums of all amino acids and of the branched chain amino acids.
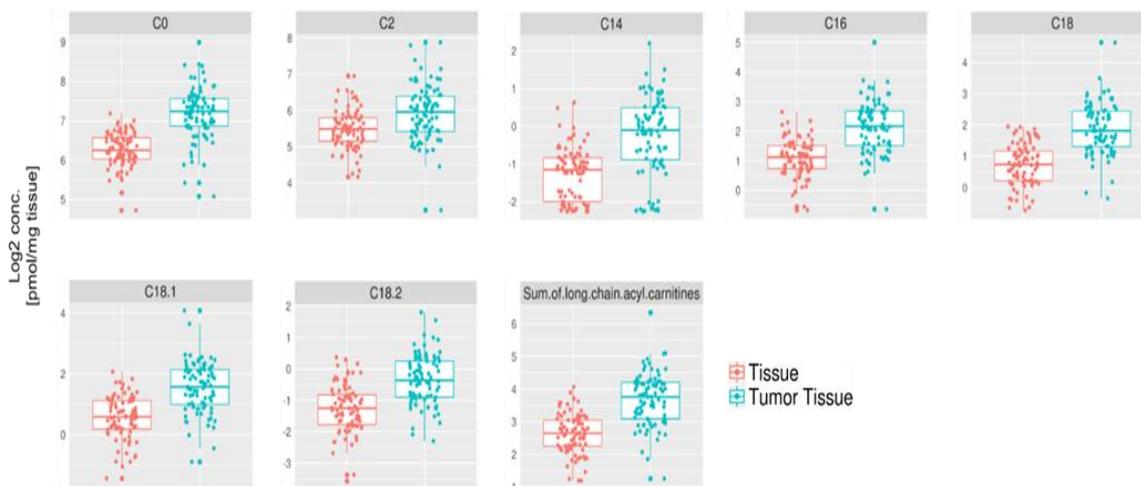
Figure 9: Significantly changed acylcarnitines.
Analytes with significantly changed concentrations between tumor and tumor-surroundingtissue, including the sum of all long chain acyl carnitines (acyl chains C14-C18).
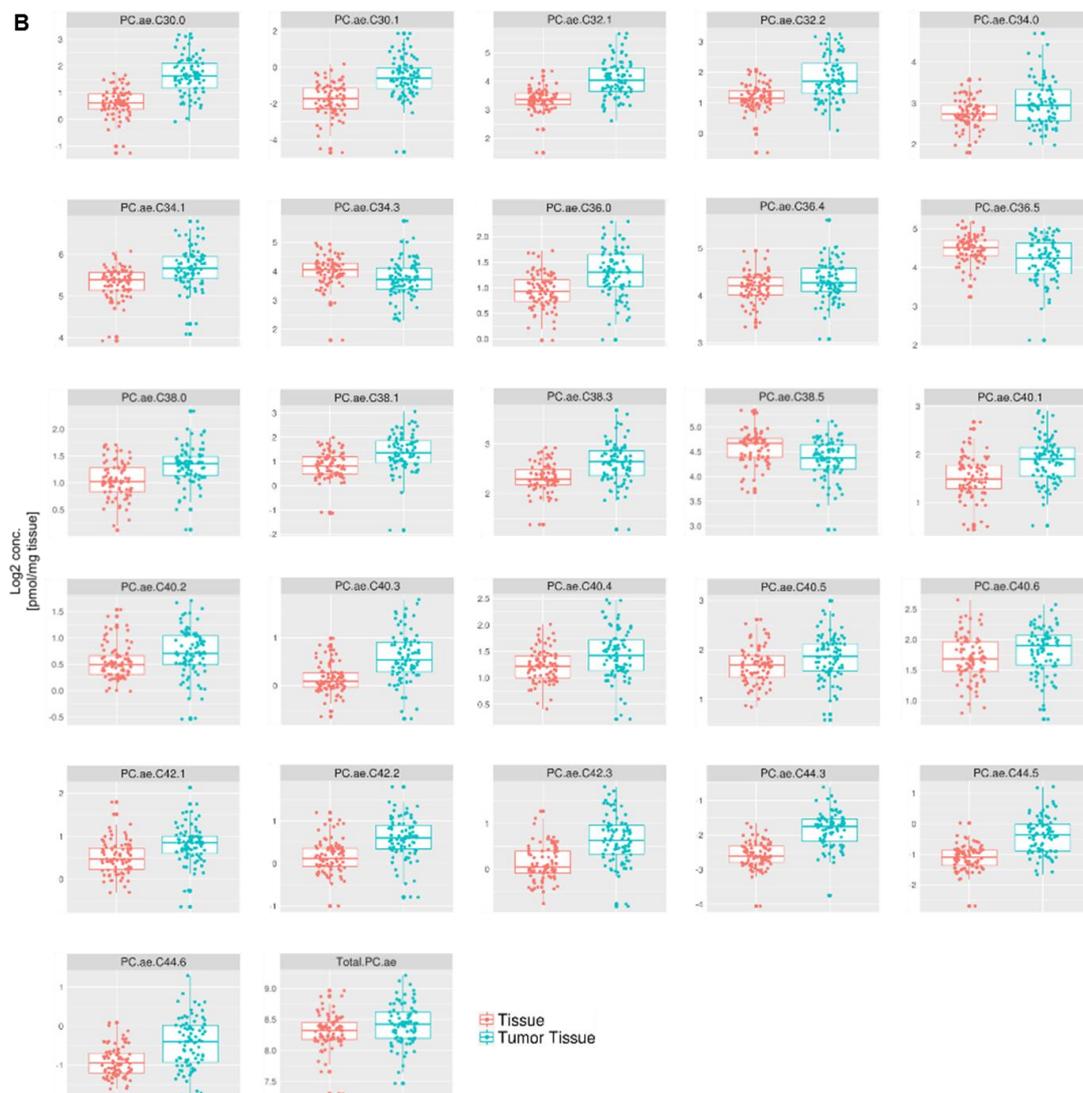
Figure 10: Significantly changed phosphatidylcholines.
A) Diacyl-phosphatidylcholineswith significantly changed concentrations between tumor and tumor-surrounding tissue.B) Acyl-alkyl-phosphatidylcholineswith significantly changed concentrations between tumor and tumor-surrounding tissue, including the sum of all acyl-alkyl-phosphatidylcholines.
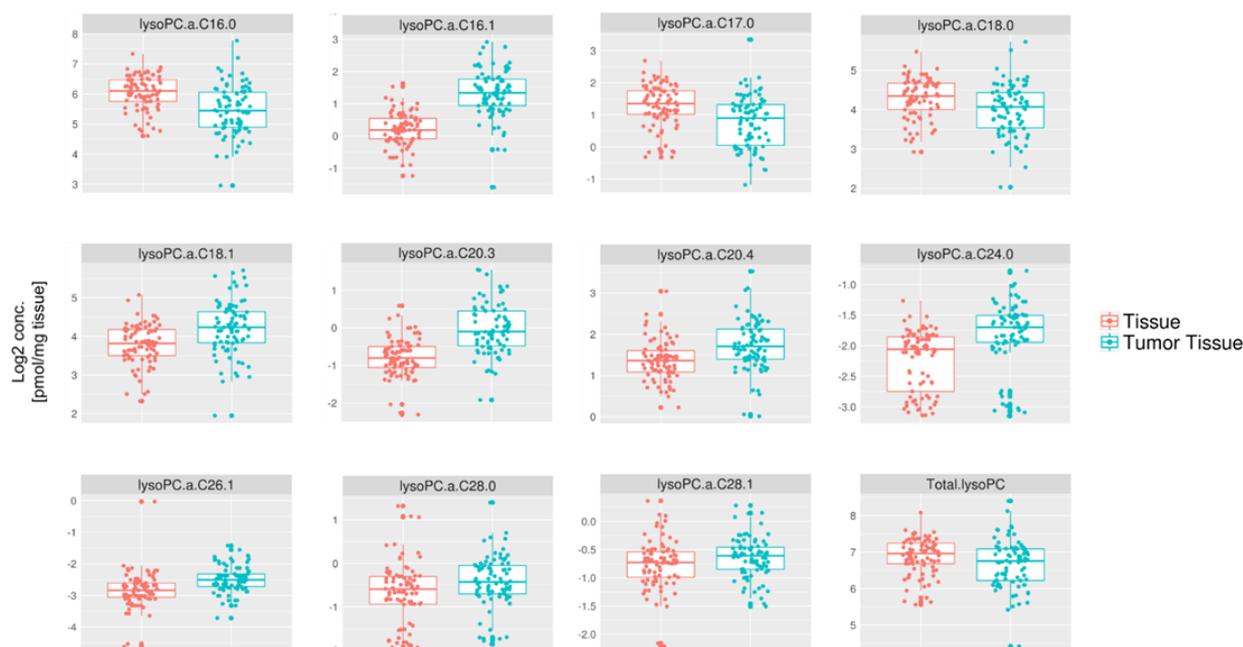
Figure 11: Significantly changed lysophosphatidylcholines.
Analytes with significantly changed concentrations between tumor and tumor-surrounding tissue, including the sum of all lysoPCs.
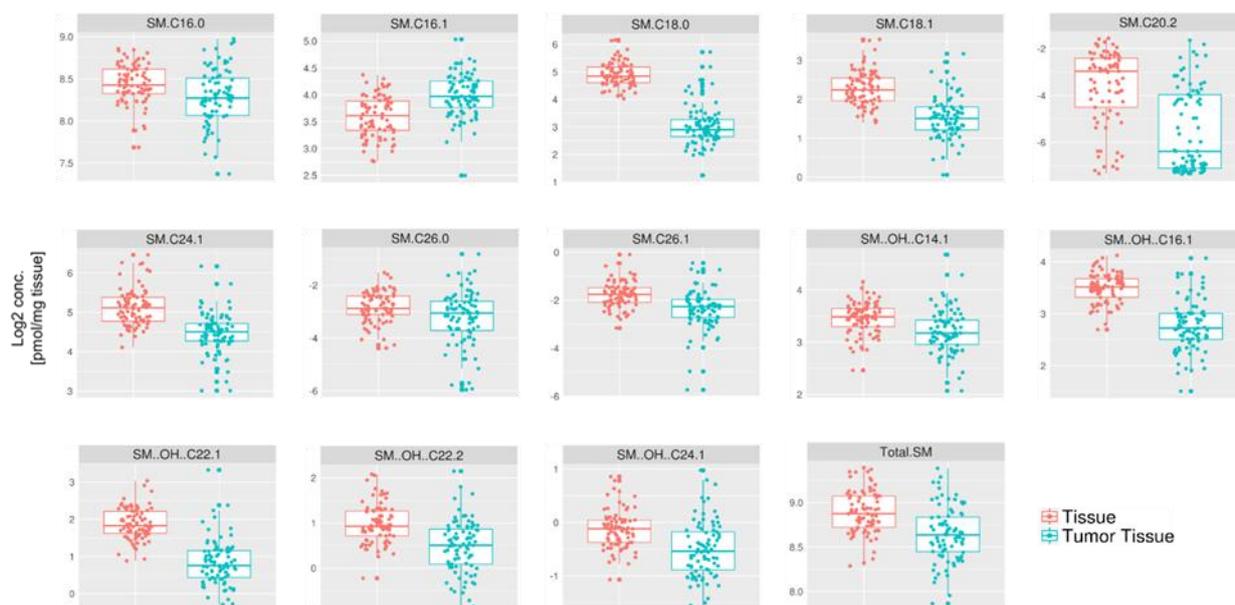

Figure 12: Significantly changed sphingomyelins.
Analytes with significantly changed concentrations between tumor and tumor-surrounding tissue, including the sum of all sphingomyelins.

The amino acid arginine forms the link between the observed elevated amino acids and the observed elevated concentrations of metabolites of the urea cycle and polyamine metabolism. Methylated arginine is a post-translational modified version of arginine that is commonly formed from protein arginine. In contrast to symmetrically (SDMA), asymmetrically methylated forms of arginine (ADMA) are toxic when released during protein turnover and have been linked to arterial stiffness and heart disease. Average concentration levels of ADMA were higher in tumor tissue, which has been reported previously by others.[15] It has been suggested that the high ADMA concentrations are beneficial for the cancer cells as they reduce susceptibility to apoptosis. Polyamines, including putrescine, spermidine, and spermine, all contain two or more primary amino groups. The biological roles for polyamines are various, including DNA binding, modulation of translation, cell growth, and ion channel receptors. Almost all cells can produce polyamines, but their production is especially high in rapidly growing cells. The capacity of cancer tissue to produce high amounts of polyamines likely

contributes to their enhanced proliferation because polyamines are indispensable for cellular growth, which may at least partially explain why cancer patients with increased polyamine levels have a poorer prognosis (16,17). A comprehensive study also found higher single and total polyamine levels in colorectal carcinoma compared to normal surrounding mucosa, correlating to the results in the present study. Opposite to putrescine and spermidine, spermine levels were reduced in the tumor tissue in the present study. Notably, tumor sperminelevels were identified as a significant prognostic factor for disease recurrence previously.[16]

Within the aromatic amino acids, especially the tryptophan pathway has been described to play a role in cancer. Kynurenine is synthesized from tryptophan by the enzyme Indoleamine-2, 3-dioxygenase (IDO) in many tissues in response to immune activation. Kynurenine and its further breakdown products have been described to be involved in diverse biological functions, such as dilating blood vessels during inflammation and regulating the immune response. Interestingly, some cancers show increased kynurenine production, which in turn enhances tumor growth. IDO permits tumor cells to escape the immune system by depletion of tryptophan in the microenvironment of the cells. Overexpression of IDO has also been found in the context of colorectal cancer.[19]

Like kynurenine, serotonin is also a tryptophan-derived metabolite. Serotonin is a biogenic amine that serves as a neurotransmitter in the central nervous system, local regulator in the gut, and vasoactive agent in the blood. Serotonin is mainly synthesized and stored in the enterochromaffin cells of the intestine. Recently it has been shown that serotonin promotes angiogenesis in colon cancer allografts by specifically influencing matrix metalloprotease expression in tumor-infiltrating macrophages, thereby affecting the production of circulating angiogenesis inhibitor angiostatin In contrast to these results, and opposite to kynurenine and tryptophan, and in fact to most amino acids and biogenic amines, the present study found serotonin levels much higher in non-tumor tissue than in tumor tissue. Consistently, the ratio corresponding to the serotonin synthesis by tryptophan hydroxylase and aromatic L-amino acid decarboxylase showed a significant reduction of the activity of these enzymes in the tumor tissue, indicating a shift in the tumor cell metabolism funneling most of the tryptophan into the kynurenine pathway, promoting tumor growth.

Likewise, the biogenic amine histamine was decreased in tumor tissue, although it is mainly derived from the essential amino acid histidine, which was detected at increased levels in the tumor tissue compared to the control. Histamine is a product of histidine decarboxylation by the enzyme histidinedecarboxylase. The present results indicate that histidine decarboxylase expression or activity was negatively affected in the

tumor tissue.Oncogene-mediated repression of histidine decarboxylase expression has been reported.[21] which contributes to maintaining high levels of histidine in the cancer cells, promoting tumor growth. However, several previous studies indicated that also histamine can modulate proliferation of different normal and malignant cells. High histamine biosynthesis and levels, together with specific histamine receptors, have been found in different human melanoma, colon, and breast cancers, as well as in experimental tumors in which histamine has been reported to act as a paracrine and autocrine regulator of proliferation, usually with a pro-proliferative effect In addition, histamine released by mast cells was described to induce tumor proliferation and immunosuppression through the specific expression of its associated histamine receptors.[23,24] The examples of glutamine, spermine, histamine, and serotonin show that although the metabolism of some ontology classes like amino acids and biogenic amines was almost completely shifted towards higher concentrations in tumor cells, the presence or activity of certain enzymes is specifically affected in the tumor tissue so that distinct metabolites show the opposite trend. In this way, small differences in the single metabolite concentrations can have a major effect on the overall cell status.

As expected, BCAAs were also detected at higher levels in the tumor tissue, as in several previous studies. BCAAs account for over 20% of total dietary protein obtained from the human diet. BCAAs have emerged as biomarkers of metabolic diseases and have the potential to predict type II diabetes.[25] Similarly, the sum of BCAAs has been used as an indicator for short-term metabolic control, mTOR signaling and insulin secretion (26). Both diabetes and cancer are characterized by severe metabolic alterations and the BCAAs appear to play a key role in both of these diseases.[27] BCAAs are enzymatically degraded by BCKDH (BCAA α-keto acid dehydrogenase) and converted to acetyl-CoA, to enter the TCA cycle. Therefore, the catabolism of BCAAs provides an important source for the generation of other amino acids, especially glutamine and alanine. These amino acids are in turn essential as an energy source or for protein synthesis in cancer cells.

In addition to amino acids and biogenic amines, acylcarnitines play a major role in the energy metabolism of cancer cells. Carnitine, which is synthesized from the amino acids lysine and methionine, is essential for the transport of long-chain acyl groups from fatty acids into the mitochondrial matrix. Inside the mitochondrial matrix, fatty acids can be broken down to acetyl-CoA in a process called β-oxidation, so they can enter the TCA cycle for energy production. The transfer of the activated fatty acid to carnitine is catalyzed by a series of reactions including the enzymes carnitine acyltransferase I, carnitine-acylcarnitine translocase, and carnitine acyltransferase II.Consistent with our results, a recent study found a variety of elevated acylcarnitine species in colon cancer cells compared to ovarian cancer cells,

potentially due to enhanced β-oxidation and energy demand.[28]

In the present study, also a lot of significant alterations in lipid concentrations were detected comparing the tumor tissue with the adjacent normal tissue. Interestingly, different classes of phospholipids displayed concentration changes in different directions: we observed increased phosphatidylcholine levels and reduced lysophosphatidylcholine and sphingomyelin levels in the tumor tissue.

Sphingomyelins are a class of sphingolipids that consist of a sphingosine backbone to which a phosphocholine moiety and a fatty acid are attached. Sphingomyelins are essential in the composition of the myelin sheath that surrounds nerve cell axons and serve as widespread membrane components. Additionally, the synthesis as well as degradation of sphingomyelins give rise to lipid soluble second messengers such as diacylglycerol or ceramides.[29] Mouse studies have previously shown that nutritional consumption of sphingolipids can inhibit colon carcinogenesis. In detail, sphingomyelin supplementation is able to reduce the number of aberrant colonic crypt foci, and upon a longer period of feeding, reduces the number of colonic adenocarcinomas. The suggested mechanism for this effectis that exogenously supplied sphingolipids counteract sphingolipid signaling defects in the cancer. Sphingolipids can act as a source for sphingosine and ceramides, which were shown to induce apoptosis in a human colorectal adenocarcinoma cell line.[30]

Phosphatidylcholines (PCs) are usually the most abundant phospholipid class in animals and are incorporated as one of the major components of membranes. PCs are composed of a choline head group, a glycerophosphoric acid together with a variety of saturated and unsaturated fatty acids.[31] PCs can be further subdivided into diacyl (aa) and acyl-alkyl (ae) PCs.

Our results are in line with previous studies, which found that the overall level of PCs is elevated in colorectal cancer. In addition to increased amounts of phospholipids, the phospholipid composition of the colorectal cancer cell membrane was altered. These changes in membrane phospholipid levels can directly influence cell proliferation, viability, and tumor development. Increased levels of monounsaturated fatty acids and monounsaturated phosphatidylcholines relative to polyunsaturated fatty acids and polyunsaturated phosphatidylcholines were also observed in the cancer microenvironment compared to the adjacent normal tissue of different cancer cell types.[32]

Lysophosphatidylcholines (lysoPCs) result from the partial hydrolysis of phosphatidyl-cholines; one fatty acid group is enzymatically removed by Phospholipase A2. The reduced lysoPC levels together with the increased PC levels in the tumor tissue detected in this study may be due to a reduced phospholipase A2 activity. Many studies have shown some impact of diverse phospholipase A2 enzymes on cancer, although whether they promote or inhibit tumor growth seems to depend on the organ and the biochemical microenvironment of the tumors.[33] LysoPCs are present as minor phospholipids in the cellular membrane and in the blood plasma. As lysoPCs are rapidly metabolized by lysophospholipase and LPC-acyltransferase, they only have a short half-life *in vivo*. Certain lysoPCs were recently described as important cellsignaling molecules.[334,35] For example, lysophosphatidic acid acts as an autocrine growth factor and is able to stimulate proliferation, adhesion, invasion, and tumor metastasis of ovarian cancer cells (36–38).

In the context of colorectal cancer, a previous study found that cancer patients had lower plasma levels of total lysoPCs, saturated lysoPCs, unsaturated lysoPCs, and lysoPCs C16:0, and C18:0.[39] These observations are in line with this study and possibly highlight lysoPCs as biomarkers for colorectal cancer. While a potential shift between lysoPC levels from blood to tumor tissue indicates an increased consumption of lysoPCs by tumor cells, specific signaling properties of lysoPCs in cancer cells remain to be elucidated.[40] Additionally, LysoPCs may also act as carriers of fatty acids, and extracellular hydrolysis of lysoPCs followed by a rapid uptake of the respective fatty acids appears to be a characteristic of solid tumors in mice.[1]

Overall, the tumor tissue samples displayed severely altered metabolomic features, which affected different pathophysiological pathways ranging from energy to lipid metabolism. Metabolomic reprogramming, glutaminolysis, the prominent Warburg Effect, and increased IDO activity, which all have been described for cancer cells,were conclusively observed in this analysis. In addition, the importance of lipid alterations in tumor cells was confirmed with this study.

A new concept of carcinogenesis recently described by Da Silva et al.[3] incorporates existing understanding of the genomic basis of cancer into a fundamentally different paradigm. The findings of the investigation suggest that cancer "conscripts" the human genome to meet its needs under conditions of systemic metabolic stress. Their studies support the hypothesis that cancer arises as a local manifestation of a state a systemic metabolic insufficiency. The authors' findings are consistent with inborn-like errors of metabolism and define a continuum from normal controls to elevated risk to invasive breast cancer. Similar results have been observed in other adenocarcinomas. A new early detection platform is described which supports a role for pre-existing, inborn-like errors of metabolism in the carcinogenesis process of all glandular malignancies. In this context,it would be interesting to compare the results from the present study to metabolomics data from colon

tissue samples of healthy patients to quantify whether the metabolic phenotype of the normal adjacent mucosa of colon cancer patients is more similar to the colon cancer patients or the healthy controls.

The current demand for personalized treatment focuses on early identification of high-risk cancers for preventive treatment, instead of later progressive curative treatment. Metabolomics of intact tissue samples could help obtain biological understanding of cancer disease, and may, eventually, extend the existing clinical tools for cancer diagnosis and treatment. Metabolic profiles of cancer tissue are distinct from the normal adjacent counterparts. High resolution magic angle spinning nuclear magnetic resonance (HR-MAS NMR)is a new technique for metabolic profiling of intact tissue samples and provides a metabolite-derived phenotypic differentiation of the cancer, by describing response or resistance patterns, which in the future may result in improved stratification of patients for personalized treatment. Biopsies from cancer and normal adjacent tissue are sufficient for the analysis with HR-MAS.[42]

The use of biomarkers for prognostic or predictive interpretation of a disease state has a long tradition in clinical medicine.MR metabolomics could be used for identification of multivariate biomarkers to aid in early detection of cancer, stratify patients for the most efficient treatment, and predict survival.[42]

Another study based on GC-MSmetabolomics was able to identify and validate a diagnostic biomarker for CRC and even detect adenomas in blood. Further testing in a screening population (where prevalence is much lower) will help determine the utility of these diagnostic biomarkers for screening. Future efforts shall be directed at developing a quantitative assay, as well as further external validation using samples from multiple centers. In addition, further biomarker development will be important in hereditary forms of CRC, as well as CRC associated with inflammatory bowel disease.[43]

Based on the results of our investigation the role of sphingomyelins and lysoPCs as potential tissue biomarkers for colorectal cancer must be further investigated. Although potential interindividual differences can be present, this study shows the dramatic metabolomic changes in tumor tissue in the context of colorectal cancer.

REFERENCES

1. Brown DG, Rao S, Weir TL, O'Malia J, Bazan M, Brown RJ, et al. Metabolomics and metabolic pathway networks from human colorectal cancers, adjacent mucosa, and stool. Cancer Metab, 2016; 4: 11.
2. Farshidfar F, Kopciuk KA, Hilsden R, Elizabeth McGregor S, Mazurak VC, Donald Buie W, et al. A quantitative multimodal metabolomic assay for colorectal cancer. BMC Cancer. BMC Cancer, 2018; 18: 12.
3. da Silva I, Vieira R da C, Stella C, Loturco E, Carvalho AL, Veo C, et al. Inborn-like errors of metabolism are determinants of breast cancer risk, clinical response and survival: a study of human biochemical individuality. Oncotarget, 2018; 9.
4. Zhang Y, Zhang F, Li K, Yang C, Hou Y, Ma L, et al. Metabolomics for biomarker discovery in the diagnosis, prognosis, survival and recurrence of colorectal cancer: a systematic review. Oncotarget, 2017; 8: 35460–72.
5. Siskos AP, Jain P, Römisch-Margl W, Bennett M, Achaintre D, Asad Y, et al. Interlaboratory Reproducibility of a Targeted Metabolomics Platform for Analysis of Human Serum and Plasma. Anal. Chem, 2017; 89: 656-665.
6. Ramsay SL, Stoegg WM, Weinberger KM, Graber A, Guggenbichler W. Apparatus and method for analyzing a metabolite profile. EP 1875401, A211-Jan-2007.
7. Di Guida R, Engel J, Allwood JW, Weber RJM, Jones MR, Sommer U, et al. Non-targeted UHPLC-MS metabolomic data processing methods: a comparative investigation of normalisation, missing value imputation, transformation and scaling. Metabolomics, 2016; 12: 93.
8. Kooperberg C, Stone CJ. Logspline Density Estimation for Censored Data. J Comput Graph Stat. Taylor & Francis; 1992;1:301–28.
9. Benjamini Y, Hochberg Y. Benjamini-1995.pdf. J R Stat Soc B., 1995; 57: 289–300.
10. Ai W, Liu Y, Langlois M, Wang TC. Kruppel-like factor 4 (KLF4) represses histidine decarboxylase gene expression through an upstream Sp1 site and downstream gastrin responsive elements.J Biol Chem, 2004 Mar 5; 279(10): 8684-93.
11. Schooneman MG, Vaz FM, Houten SM, Soeters MR. Acylcarnitines: reflecting or inflicting insulin resistance? Diabetes, 2013; 62: 1–8.
12. Lunt SY, Vander Heiden MG. Aerobic Glycolysis: Meeting the Metabolic Requirements of Cell Proliferation. Annu Rev Cell Dev Biol, 2011; 27: 441–64.
13. Chen J-Q, Russo J. Dysregulation of glucose transport, glycolysis, TCA cycle and glutaminolysis by oncogenes and tumor suppressors in cancer cells. Biochim Biophys Acta - Rev Cancer, 2012; 1826: 370–84.
14. Jin L, Alesi GN, Kang S. Glutaminolysis as a target for cancer therapy. Oncogene, 2016; 35: 3619–25.
15. Kim MH, Kim H. Oncogenes and Tumor Suppressors Regulate Glutamine Metabolism in Cancer Cells. J Cancer Prev., 2014; 18: 221–6.
16. Li H. et al.. Asymmetric dimethylarginine attenuates serum starvation-induced apoptosis via suppression of the Fas (APO-1/CD95)/JNK (SAPK) pathway. Cell Death Dis, 2013; 4: e830.
17. Linsalata, M., Caruso, M. G., Leo, S., Guerra, V., D'Attoma, B., & Di Leo A. Prognostic value of

tissue polyamine levels in human colorectal carcinoma. Anticancer Res., 2002; 22: 2465–9.

18. Bergeron C, Bansard J, Le Moine P, Bouet F, Goasguen J, Moulinoux J, et al. Erythrocyte spermine levels: a prognostic parameter in childhood common acute lymphoblastic leukemia. Leukemia, 1997; 11: 31–6.

19. Godin-Ethier J, Hanafi L-A, Piccirillo CA, Lapointe R. Indoleamine 2,3-Dioxygenase Expression in Human Cancers: Clinical and Immunologic Perspectives. Clin Cancer Res., 2011; 17: 6985–91.

20. Uyttenhove C, Pilotte L, Théate I, Stroobant V, Colau D, Parmentier N, et al. Evidence for a tumoral immune resistance mechanism based on tryptophan degradation by indoleamine 2,3-dioxygenase. Nat Med, 2003; 9: 1269–74.

21. Nocito A, Dahm F, Jochum W, Jang JH, Georgiev P, Bader M, et al. Serotonin Regulates Macrophage-Mediated Angiogenesis in a Mouse Model of Colon Cancer Allografts. Cancer Res, 2008; 68: 5152–8.

22. Lampiasi N, Azzolina A, Montalto G, Cervello M. Histamine and spontaneously released mast cell granules affect the cell growth of human hepatocellular carcinoma cells. Exp Mol Med, 2007; 39: 284–94.

23. Dyduch G, Kaczmarczyk K, Okoń K. Mast cells and cancer: enemies or allies? Pol J Pathol, 2012; 63: 1–7.

24. Fang Z, Yao W, Xiong Y, Li J, Liu L, Shi L, et al. Attenuated expression of HRH4 in colorectal carcinomas: a potential influence on tumor growth and progression. BMC Cancer, 2011; 11: 195.

25. Chen X, Yang W. Branched-chain amino acids and the association with type 2 diabetes. J Diabetes Investig, 2015; 6: 369–70.

26. Neinast M, Murashige D, Arany Z. Branched Chain Amino Acids. Annu Rev Physiol, 2019 Feb 10; 81: 139-164.

27. Calle EE, Kaaks R. Overweight, obesity and cancer: epidemiological evidence and proposed mechanisms. Nat Rev Cancer, 2004; 4: 579–91.

28. Halama A, Guerrouahen BS, Pasquier J, Diboun I, Karoly ED, Suhre K, et al. Metabolic signatures differentiate ovarian from colon cancer cell lines. J Transl Med, 2015; 13: 223.

29. Slotte JP. Biological functions of sphingomyelins. Prog Lipid Res., 2013; 52: 424–37.

30. Berra B, Colombo I, Sottocornola E, Giacosa A. Dietary sphingolipids in colorectal cancer prevention. Eur J Cancer Prev, 2002; 11: 193–7.

31. Cole LK, Vance JE, Vance DE. Phosphatidylcholine biosynthesis and lipoprotein metabolism. Biochim Biophys Acta - Mol Cell Biol Lipids, 2012; 1821: 754–61.

32. Guo S, Wang Y, Zhou D, Li Z. Significantly increased monounsaturated lipids relative to polyunsaturated lipids in six types of cancer microenvironment are observed by mass spectrometry imaging. Sci Rep, 2014; 4: 1–9.

33. Scott KF, Sajinovic M, Hein J, Nixdorf S, Galettis P, Liauw W, et al. Emerging roles for phospholipase A2 enzymes in cancer.Biochimie, 2010 Jun; 92(6): 601-10.

34. Moolenaar WH, van Meeteren LA, Giepmans BNG. The ins and outs of lysophosphatidic acid signaling. BioEssays, 2004; 26: 870–81.

35. Xu Y, Xiao Y, Zhu K, Baudhuin L, Lu J, Hong G, et al. Unfolding the Pathophysiological Role of Bioactive Lysophospholipids. Curr Drug Target - Immune, Endocr Metab Disord, 2003; 3: 23–32.

36. Mills GB, Moolenaar WH. The emerging role of lysophosphatidic acid in cancer. Nat Rev Cancer. 2003;3:582–91.

37. Xu Y, Shen Z, Wiper DW, Wu M, Morton RE, Elson P, et al. Lysophosphatidic acid as a potential biomarker for ovarian and other gynecologic cancers. JAMA, 1998; 280: 719–23.

38. Ren J, Xiao Y, Singh LS, Zhao X, Zhao Z, Feng L, et al. Lysophosphatidic Acid Is Constitutively Produced by Human Peritoneal Mesothelial Cells and Enhances Adhesion, Migration, and Invasion of Ovarian Cancer Cells. Cancer Res., 2006; 66: 3006–14.

39. Casey G, Tan H, Berk M, Xiao Y, Zhao Z, Li L, et al. Plasma Lysophosphatidylcholine Levels: Potential Biomarkers for Colorectal Cancer. J Clin Oncol, 2007; 25: 2696–701.

40. Lee KB, Joo EJ, Linhardt RJ, Li L, Gasimli L, Weyers A, et al. Carbohydrate-Containing Molecules as Potential Biomarkers in Colon Cancer. Omi A J Integr Biol, 2014; 18: 231–41.

41. Raynor A, Jantscheff P, Ross T, Schlesinger M, Wilde M, Haasis S, et al. Saturated and mono-unsaturated lysophosphatidylcholine metabolism in tumour cells: A potential therapeutic target for preventing metastases. Lipids Health Dis. Lipids in Health and Disease, 2015; 14: 1–15.

42. Bathen TF, Sitter B, Sjøbakk TE, Tessem MB, Gribbestad IS. Magnetic resonance metabolomics of intact tissue: A biotechnological tool in cancer diagnostics and treatment evaluation. Cancer Res., 2010; 70: 6692–6.

43. Farshidfar F, Weljie AM, Kopciuk KA, Hilsden R, McGregor SE, Buie WD, et al. A validated metabolomic signature for colorectal cancer: exploration of the clinical value of metabolomics. Br J Cancer. The Author(s), 2016; 115: 848.